JOURNAL OF SOLID STATE CHEMISTRY 47, 185–200 (1983)

A Crystal Chemical Study of Stishovite

R. J. HILL

CSIRO Division of Mineral Chemistry, Port Melbourne, Victoria, Australia

M. D. NEWTON

Department of Chemistry, Brookhaven National Laboratory, Upton, New York 11973

AND G. V. GIBBS

Department of Geological Sciences, Virginia Polytechnic Institute and State University, Blacksburg, Virginia 24061

Received April 6, 1982; in final form November 20, 1982

The crystal structure of stishovite, SiO_2, $a = 4.1773(1)$, $c = 2.6655(1)$ Å, space group $P4_2/mnm$, with $Z = 2$, has been refined with 217 graphite-monochromatized Mo$K\alpha$ data (2θ max = 120°) to $R = 0.012$ ($R_w = 0.014$). Electron deformation density maps show a modest accumulation of charge density ascribed to partial covalent bonding in both the equatorial and axial bonds together with a delocalization of density in and around the shared octahedron edges with the shorter equatorial bonds showing higher peaks (0.47 e Å^{-3}) than the longer axial bonds (0.29 e Å^{-3}). Net atomic charges for Si and O determined by a population and κ refinement by varying the occupancy and shape of their valence shells are +1.71 and −0.86(15) e, respectively. The observed structural distortions and charge distributions conform with the results of *ab initio* molecular orbital calculations undertaken on molecules designed to mimic the local geometry of the structure of stishovite. The Si–O bond length (1.73 Å) calculated for a neutral molecule with 6-coordinated Si is slightly shorter than that observed on the average (1.76 Å) for silicates and molecular crystals with 6-coordinated Si. In addition, the calculated geometrical parameters of two edge-sharing octahedra agree to within ~5% of the observed geometry of stishovite. The calculated charge on Si is indicated to increase with coordination number and bond length in agreement with the larger net charge recorded for stishovite as compared with that recorded for α-quartz, Q(Si) = +1.0 e. Observed deformation maps are compared with theoretical ones calculated in the equatorial plane of the 6-coordinated molecule using molecular orbital theory with a split valence s,p basis supplemented with d-type polarization functions on Si.

Introduction

Whereas the chemistry of the animal and vegetable worlds is dominated by carbon, oxygen, and hydrogen, that of the world of minerals is almost completely dominated by silicon and oxygen. Indeed, almost 60%, by weight, of the Earth's continental crust, and more than 45% of the oceanic crust and mantle, consists of the component oxide SiO_2. It is, therefore, not surprising that a detailed knowledge of the properties of the

0022-4596/83 $3.00

Si–O bond is of central importance in attempts to understand inorganic materials in the natural environment.

The polymorphs of SiO_2 are of particular interest, not only because they constitute some 12 wt% of the entire crust (chiefly as the mineral α-quartz in igneous rocks), but also because they are among the most common and utilitarian materials in human society and its technology. As a result, the literature abounds with experimental and theoretical studies devoted to the elucidation of the crystal and electronic structures of these dozen or so forms of silicon dioxide (see, for examle, the reviews by Griscom (*1*), Hubner (*2*), Pantelides (*3*), Newton and Gibbs (*53*), and Gibbs *et al.* (*4, 5*)). However, in all but one of these polymorphs the silicon atoms are surrounded by an approximately tetrahedral array of oxygen atoms, where each oxygen is bonded to two silicon atoms. Understandably, therefore, the vast majority of previous work has concentrated on the properties of silicon tetrahedrally coordinated by oxygen.

The exception to the rule is the mineral stishovite, first synthesized at high pressure and temperature in the laboratory (*6*), and later discovered in an impact breccia at Meteor Crater, Arizona (*7*). In this structure each silicon atom is coordinated by six oxygen atoms in octahedral configuration, and each oxygen is bonded to three silicon atoms. As a result of its higher coordination numbers and its shorter O . . . O nonbonded contacts relative to those in the other silica polymorphs, the density of stishovite (4.28 g cm^{-3}) is some 46% greater than that of the densest of the 4-coordinated polymorphs (coesite), and it has therefore been suggested to be one of the predominant phases at depth in the Earth's mantle, produced either by transformation of α-quartz or as a disproportionation product of common silicate minerals (*8*). Octahedral coordination of silicon by oxygen has also been observed in a number of other high pressure structure types including hollandite (*9, 10*), garnet (*11*), and perovskite (*12*), but it is not unknown in phases formed at low pressure. In fact, the synthesis of solids with 6-coordinate Si at low pressures is possible and well documented (*13–17*). However, in these cases the other atoms bonded to the coordinating oxygen atoms are atoms of relatively high electronegativity like (*15, 18*) carbon, as in the recent report of 6-coordinate Si in two molecular crystals (*19*). Stishovite itself, however, remains the most attractive candidate for a detailed study of 6-coordinated silicon, firstly because of its chemical simplicity, and secondly because of its direct relevance to studies of the geophysics and mineralogy of the mantle.

Earlier structural studies of stishovite were based on powder X-ray diffraction data (*20–22*), but the recent synthesis of crystals up to 0.23 mm in length have, for the first time, enabled the precise determination of its structure from single crystal data (*23*). In the present work we extend the analysis of stishovite in two ways: (i) the X-ray scattering formalism embodied in the usual least-squares refinement procedure has been made more flexible by the incorporation of parameters representing variable occupancy and expansion/contraction of the atomic valence shell (*24*), thereby allowing an estimation of net atomic charges on Si and O and the deformation density, and (ii) the experimental results are compared with those from *ab initio* molecular orbital calculations undertaken on molecules designed to mimic the stishovite structure in an attempt to rationalize the observed bond and shared-edge lengths, valence angles, and electron deformation density distribution.

Experimental

Crystals of stishovite synthesized by the method described in Ref. (*23*) were kindly

made available for study by Mr. W. Sinclair and Professor A. E. Ringwood of the Research School of Earth Sciences at the Australian National University. The crystal selected for data collection was a transparent rectangular {110} prism, of length 0.082 mm and base 0.078 × 0.052 mm, terminated by pyramidal faces of the form {111}. The specimen was mounted on a Philips PW1100 four-circle automatic diffractometer in an arbitrary orientation and the unit cell parameters refined by a least-squares technique from the observed 2θ values of 25 automatically centered reflections in the range 2θ = 106–116°, measured at 22°C with Mo $K\alpha_1$ radiation (λ = 0.70930 Å). The resultant tetragonal cell dimensions, a = 4.1773(1) and c = 2.6655(1) Å, are in close agreement with those determined on the same material by Sinclair and Ringwood (*23*), and with previous powder X-ray diffraction measurements (*7, 25*).

Intensity data for the structure analysis were collected with Mo $K\alpha$ radiation monochromated by a flat graphite crystal ($2\theta_m$ = 12.17°) using a θ–2θ scan technique and a 2θ scan rate of 2° min^{-1}. Backgrounds were determined from 20-sec stationary counts at both ends of each dispersion-modified ($\Delta 2\theta$ = 1.8 + 0.76 tan θ) scan range. All 2780 reciprocal lattice points within a sphere of radius 1.22 Å^{-1} ($2\theta_{max}$ = 120°) were sampled, but the last 20% of the data was subsequently deleted due to X-ray tube softening and eventual failure. Up to this point three noncoplanar reflections monitored every 60 min showed no significant variation in either intensity or position. The resultant 2173 reflections were corrected for background, Lorentz, and polarization effects using a program written specifically for the PW1100 diffractometer (*26*). Since the plane of reflection of the graphite monochromator was perpendicular to that of the specimen crystal, the Lorentz–polarization correction was of the form $(Lp)^{-1} = \sin 2\theta\,(1 + \cos^2 2\theta_m)/(\cos^2 2\theta + \cos^2 2\theta_m)$. Absorption corrections were then applied to the data with the Gaussian quadrature method as coded in the XRAY76 system of programs (*27*) using a 6 × 6 × 6 grid and a μ value of 15.72 cm^{-1}: the minimum and maximum transmission factors were 0.887 and 0.926, respectively. Multiply measured and symmetry-equivalent reflections consistent with point group *4/mmm* were then averaged to yield a set of 221 unique structure factors, F_o, each with a standard deviation estimated from the expression

$$\sigma_{F_o} = \sigma_I^2 + (0.03I^2)^{0.5}/2I^{0.5}$$

where I is the corrected raw intensity and σ_I is derived from counting and averaging statistics (Table I). The overall internal consistency factor between averaged intensities was 0.023 and only four were considered to be "unobserved" at the $1\sigma_I$ level.

Refinement

The refinement of the structure was initiated in space group symmetry $P4_2/m2_1/n2/m$ with the atomic positions and thermal[1] parameters determined by Sinclair and Ringwood (*23*), using the modified full-matrix least-squares program RADIEL (*24*). All scattering factors (including both real and imaginary anomalous dispersion components) were obtained from "International Tables for X-ray Crystallography" (*28*) and were normalized to one electron. Si and O were assigned core-scattering factors equivalent to Ne and He configurations, respectively, while their valence form factors were calculated as weighted averages (based on neutral atom electronic configurations) of the appropriate ground state orbital scattering factors.

[1] The anisotropic ellipsoids were converted to the form

$$\exp[-2\pi^2(U_{11}h^2a^{*2} + U_{22}k^2b^{*2} + U_{33}l^2c^{*2} + 2U_{12}hka^*b^* + 2U_{13}hla^*c^* + 2U_{23}klb^*c^*)].$$

TABLE I

OBSERVED STRUCTURE FACTORS F_o, AND THEIR ESD'S σ_F FOR STISHOVITE

h	k	l	F_o	σ_F	h	k	l	F_o	σ_F	h	k	l	F_o	σ_F
0	0	2	325.18	3.33	4	1	0	141.93	0.74	6	0	2	161.83	0.86
0	0	4	221.54	3.25	4	1	1	185.48	0.68	6	0	4	116.09	0.92
0	0	6	137.72	2.10	4	1	2	113.93	0.43	6	1	0	83.47	0.49
1	0	1	169.16	0.86	4	1	3	126.56	0.68	6	1	1	114.73	0.44
1	0	3	140.77	1.05	4	1	4	83.12	0.50	6	1	2	76.04	0.33
1	0	5	64.34	0.63	4	1	5	72.05	0.47	6	1	3	82.44	0.50
1	1	0	267.99	1.93	4	2	0	179.78	0.93	6	1	4	61.27	0.44
1	1	1	243.11	1.24	4	2	1	86.75	0.34	6	1	5	50.74	0.39
1	1	2	232.29	1.19	4	2	2	146.13	0.54	6	2	0	89.99	0.52
1	1	3	117.74	0.89	4	2	3	64.24	0.42	6	2	1	56.56	0.28
1	1	4	140.31	1.06	4	2	4	87.46	0.52	6	2	2	73.29	0.33
1	1	5	75.80	0.68	4	2	5	48.40	0.41	6	2	3	48.61	0.41
1	1	6	76.45	0.67	4	3	0	61.97	0.38	6	2	4	44.80	0.41
2	0	0	42.15	0.35	4	3	1	182.43	0.67	6	2	5	36.51	0.38
2	0	2	94.57	0.50	4	3	2	53.28	0.26	6	3	0	39.70	0.37
2	0	4	50.09	0.54	4	3	3	130.20	0.71	6	3	1	152.27	0.58
2	0	6	13.51	1.09	4	3	4	40.77	0.41	6	3	2	36.04	0.28
2	1	0	185.35	0.95	4	3	5	80.75	0.49	6	3	3	120.10	0.67
2	1	1	274.72	0.99	4	4	0	149.83	1.12	6	3	4	29.39	0.44
2	1	2	101.52	0.38	4	4	1	106.38	0.59	6	4	0	116.80	0.65
2	1	3	195.08	1.01	4	4	2	124.78	0.68	6	4	1	74.11	0.33
2	1	4	61.80	0.41	4	4	3	88.43	0.74	6	4	2	102.11	0.42
2	1	5	110.18	0.62	4	4	4	81.44	0.71	6	4	3	64.50	0.45
2	1	6	42.39	0.39	4	4	5	66.21	0.62	6	4	4	74.20	0.47
2	2	0	316.69	2.28	5	0	1	51.39	0.35	6	5	0	18.22	0.58
2	2	1	92.37	0.49	5	0	3	23.54	0.61	6	5	1	47.23	0.29
2	2	2	265.69	1.36	5	0	5	1.67	8.71 L	6	5	2	16.27	0.46
2	2	3	48.48	0.49	5	1	0	204.91	1.06	6	5	3	34.16	0.42
2	2	4	167.42	1.25	5	1	1	22.89	0.25	6	5	4	14.17	0.67
2	2	5	34.07	0.58	5	1	2	172.87	0.64	6	6	0	96.64	0.80
2	2	6	102.03	0.81	5	1	3	17.69	0.52	6	6	1	54.05	0.42
3	0	1	317.03	1.62	5	1	4	115.59	0.65	6	6	2	86.20	0.52
3	0	3	235.97	1.71	5	1	5	12.76	0.86	6	6	3	48.70	0.55
3	0	5	149.67	1.14	5	2	0	13.07	0.53	7	0	1	157.86	0.84
3	1	0	178.79	0.92	5	2	1	224.32	0.82	7	0	3	128.30	1.00
3	1	1	88.59	0.34	5	2	2	10.83	0.63	7	1	0	88.94	0.52
3	1	2	156.22	0.57	5	2	3	171.32	0.91	7	1	1	66.20	0.31
3	1	3	54.42	0.37	5	2	4	10.35	1.02	7	1	2	75.38	0.34
3	1	4	85.61	0.51	5	2	5	116.75	0.65	7	1	3	58.12	0.43
3	1	5	37.60	0.41	5	3	0	54.42	0.37	7	1	4	51.63	0.41
3	1	6	43.05	0.38	5	3	1	15.36	0.35	7	2	0	43.20	0.39
3	2	0	58.28	0.34	5	3	2	39.90	0.26	7	2	1	61.44	0.30
3	2	1	114.05	0.43	5	3	3	10.50	1.20	7	2	2	40.75	0.29
3	2	2	47.74	0.23	5	3	4	13.86	0.79	7	2	3	43.42	0.41
3	2	3	73.53	0.44	5	3	5	8.32	3.02	7	2	4	33.14	0.41
3	2	4	30.89	0.40	5	4	0	18.32	0.49	7	3	0	141.25	0.77
3	2	5	29.02	0.44	5	4	1	108.49	0.43	7	3	1	33.94	0.29
3	2	6	22.24	0.46	5	4	2	15.89	0.43	7	3	2	127.06	0.50
3	3	0	287.93	2.08	5	4	3	79.35	0.50	7	3	3	29.61	0.44
3	3	1	32.33	0.29	5	4	4	13.93	0.74	7	3	4	97.05	0.55

TABLE I—*Continued*

h	k	l	F_o	σ_F	h	k	l	F_o	σ_F	h	k	l	F_o	σ_F
3	3	2	240.03	1.23	5	4	5	50.80	0.38	7	4	0	63.13	0.44
3	3	3	25.60	0.54	5	5	0	189.91	1.41	7	4	1	88.63	0.38
3	3	4	161.19	1.21	5	5	1	4.42	4.37 L	7	4	2	58.86	0.31
3	3	5	19.69	0.76	5	5	2	170.16	0.90	7	4	3	72.10	0.46
4	0	0	222.42	1.61	5	5	3	3.14	7.15 L	7	5	0	32.77	0.43
4	0	2	187.71	0.97	5	5	4	130.84	1.01	7	5	1	8.57	1.88
4	0	4	116.61	0.91	6	0	0	186.94	1.38	7	5	2	27.79	0.32
7	5	3	6.29	2.81	8	2	3	16.06	0.63	9	1	0	71.10	0.47
7	6	0	47.28	0.40	8	3	0	8.76	2.62	9	1	1	64.96	0.31
7	6	1	91.93	0.38	8	3	1	15.81	0.48	9	1	2	64.42	0.33
7	6	2	44.63	0.28	8	3	2	8.27	1.09	9	2	0	45.44	0.40
7	7	0	80.59	0.69	8	3	3	7.76	1.51	9	2	1	63.16	0.31
7	7	1	36.83	0.37	8	4	0	60.14	0.43	9	2	2	42.16	0.29
8	0	0	12.90	1.11	8	4	1	23.57	0.35	9	3	0	65.09	0.44
8	0	2	8.97	1.43	8	4	2	54.14	0.31	9	3	1	32.78	0.29
8	0	4	2.58	8.28 L	8	4	3	20.37	0.48	9	3	2	59.40	0.31
8	1	0	24.29	0.48	8	5	0	8.55	2.37	9	4	0	62.12	0.42
8	1	1	108.79	0.44	8	5	1	124.27	0.48	9	4	1	63.61	0.30
8	1	2	22.71	0.39	8	5	2	6.01	2.29	10	0	0	114.20	0.89
8	1	3	89.68	0.53	8	6	0	29.03	0.41	10	1	0	21.71	0.47
8	2	0	138.33	0.75	8	6	1	12.10	0.59	10	1	1	37.34	0.26
8	2	1	17.18	0.44	9	0	1	71.21	0.47					
8	2	2	126.22	0.53	9	0	3	60.77	0.57					

Note. L indicates that the reflection is unobserved at the 1 σ_I level.

Conventional Refinement

With core and valence populations fixed at values appropriate to neutral atom configurations, the positional and thermal parameters of the two atoms in the asymmetric unit were refined by least-squares minimization of the function $\Sigma w(|F_o| - |F_c|)^2$, where F_o and F_c are the observed and calculated structure factors respectively, and $w = 1/\sigma^2_{F_o}$. Inclusion of an isotropic extinction parameter (type I, Lorentzian), as defined and scaled by Coppens and Hamilton (*29*), resulted in convergence at conventional R and R_w values of 0.013 and 0.021, respectively, with a goodness-of-fit parameter of 3.324. Further details of the refinement are given in Tables II and III; the results are essentially identical with those obtained by Sinclair and Ringwood (*23*).

As expected, the structural parameters obtained from a refinement of the high-angle data ($\sin\theta/\lambda > 0.65$ Å^{-1}) were identical, at the 2σ level, with those obtained from the full-data refinement. This result is consistent with similar studies of other topologically close-packed compounds in which the atoms are in largely symmetric bonding environments of high coordination number (*30–32*), but may be contrasted with many of the simple organic molecular compounds in which small but systematic shifts of the atoms away from their true positions, together with decreases in thermal vibration parameters, are observed when the low-angle data are ignored (*33*).

Population and κ Refinement

With the net charge in the crystal constrained to be zero, the valence shell popu-

TABLE II

SUMMARY OF LEAST-SQUARES REFINEMENTS

Refinement	Conventional (neutral atoms)	Valence population and κ
sin θ/λ max	1.22 Å^{-1}	1.22 Å^{-1}
No. of observations	217	217
No. of unobserveds	4	4
No. of variables	9	12
R	0.013	0.012
R_w	0.021	0.014
R_{F^2}	0.030	0.027
R_{wF^2}	0.045	0.029
$\Sigma w(\|F_o\| - \|F_c\|)^2$	2298	1059
Goodness of fit	3.32	2.28
Scale factor k	4.49(2)	4.58(2)
Extinction parameter[a]	0.093(4) × 10^{-4}	0.105(4) × 10^{-4}

[a] Figures in parenthesis here and elsewhere in the tables and figures represent the ESD in terms of the least significant figure to the left.

TABLE III

FRACTIONAL ATOMIC COORDINATES, POPULATION PARAMETERS, AND TEMPERATURE FACTOR COEFFICIENTS

Atom	Parameter	Conventional refinement	Valence pop^n/κ refinement
Si	$x = y = z$	0.0	0.0
	$U_{11} = U_{22}$	0.00235(6)	0.00253(6)
	U_{33}	0.00177(9)	0.00196(8)
	$U_{13} = U_{23}$	0.0	0.0
	U_{12}	0.00014(4)	0.00014(3)
	valence pop^n	4.0	2.29
	κ	1.0	1.11(8)
O	$x = y$	0.30608(6)	0.30616(4)
	z	0.0	0.0
	$U_{11} = U_{22}$	0.00306(7)	0.00327(7)
	U_{33}	0.00231(11)	0.00248(9)
	$U_{13} = U_{23}$	0.0	0.0
	U_{12}	−0.00094(7)	−0.00095(5)
	valence pop^n	6.0	6.86(15)
	κ	1.0	0.961(8)

lation parameters of both atoms were refined, together with all previous variables, using the full data set of 217 observed reflections. After 4 cycles, the valence-shell expansion/contraction parameter κ was also added, but the parameter shifts (when small) began to oscillate. Convergence was eventually achieved with the application of 66% damping factors on all parameters. Although the thermal and positional parameters changed by less than 3σ during this refinement, R_w and the goodness-of-fit

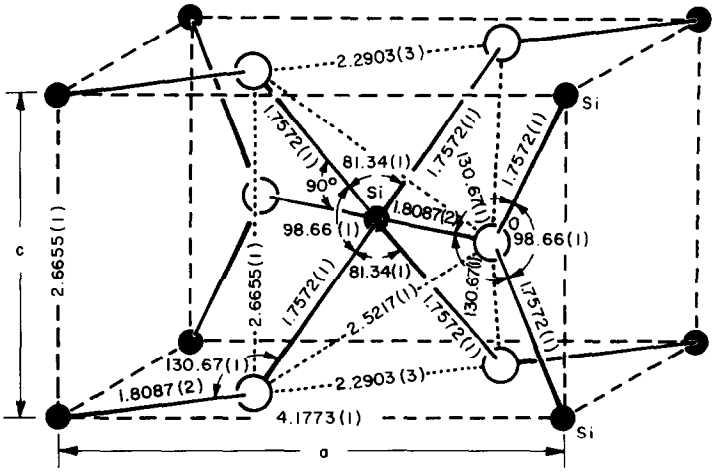

FIG. 1. Unit-cell diagram of the stishovite crystal structure drawn with the program ORTEP (*36*). Silicon–oxygen interactions are indicated by solid lines, and selected edges of the central octahedron of oxygen atoms by dotted lines. All distances and angles are in angstroms and degrees, respectively.

parameter dropped significantly to values of 0.014 and 2.279, respectively. Using Hamilton's R-factor level of significance test (*34*), the hypothesis that there is no improvement in R_w as a function of the population and κ refinement can be rejected at the conservative 0.005 confidence level ($R_{3,205,\ 0.005} < 1.05$), and we are therefore justified in discussing the results of the refinement in detail. The detailed results are collected in Tables II and III.

Discussion

Structure

Stishovite crystallizes with the well known rutile-type (C4) structure (*35*) with the bond lengths, nonbonded separations, and valence angles summarized in Fig. 1. In this structure, octahedra of anions around cations share opposite edges to form chains running parallel to the z axis. Each chain is connected sideways to four other neighboring chains by corner sharing so that each anion in the structure is coordinated by three cations.

For a C4-type structure consisting of completely regular octahedra, the two independent geometric parameters, namely the ratio of the two cell edges (c/a) and the single anion positional parameter (x), have values of $c/a = 2x = (1 + 1/\sqrt{2})^{-1} = 0.5858$. However, studies of (strictly tetragonal) C4-type oxides and fluorides (*22, 37, 38*) have shown that the angles subtended by the shared octahedral edges at the central cation are closed up[2] to the range 75–84°, while the ratio of the length of the four bonds in the (110) "equatorial" plane of the central octahedron to the length of the two "axial" bonds varies from 0.97 to 1.06. As a result, the observed values of c/a and x are increased to 0.626–0.708, and 0.301–0.310, respectively.

The narrowing down of the valence angles opposite the shared edges, together with the shortening of the edges themselves, is generally explained in terms of the competition between cation–cation and anion–anion electrostatic interactions across and along the shared edges (*39, 40*). However, this same ionic model predicts that the ratio between the equatorial and axial bond lengths should always be greater than unity (*40*). The case of stishovite (Fig. 1) is particularly interesting in this regard since the equatorial bonds are some 0.05 Å (3%) *shorter* than the axial bonds. Furthermore, the nonbonded O . . . O separation in the shared edge (2.29 Å) is considerably shorter than twice the traditional ionic radius of oxygen (2.64–2.80 Å), and ranks among the shortest of the nonbonded O . . . O separations observed in a variety of oxides (*41*). As a matter of fact, the shortening of O . . . O contacts with increasing coordination number must not be overlooked in explaining why the density of stishovite is 46% greater than that of coesite.

Although some of the geometric irregularities of the (transition-metal) C4-type oxides can be related either to asymmetries in the d-orbital occupation or to the occurrence of metallic conductivity (*37, 38*), it is clear that a complete understanding of the characteristics of this structure type will only come from a detailed knowledge of the total electron density distribution.

Electron Density Maps

The effect of chemical bonding on the electron density distribution of the atoms in a crystal may be conveniently displayed by the Fourier transform of the differences between the observed and calculated structure factors

[2] Exceptions to this rule occur for those compounds in which there is metal–metal bonding across the shared octahedron edges, resulting in an increase in both the edge length and angle (*37*).

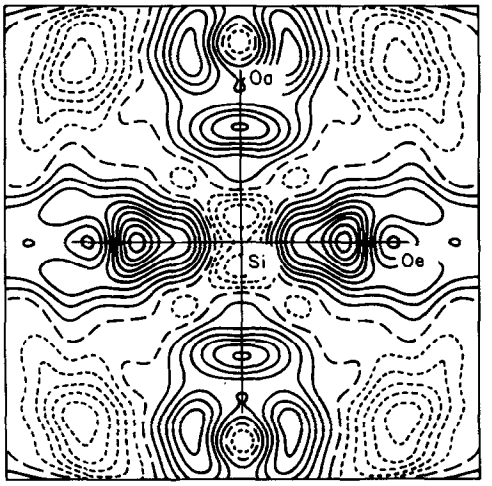

FIG. 2. Experimental deformation density map for the octahedron axial/equatorial bond plane in stishovite calculated with atomic parameters from the full-data population/κ refinement using a data cutoff of 1.0 Å^{-1}. The contour interval is 0.05 e Å^{-3}; negative and zero contours are short dashed and long dashed, respectively.

$$\Delta\rho = \frac{1}{V}\sum_{hkl}(F_o/k - F_s)\exp\{-2\pi i(hx + ky + lz\}$$

where F_s is the structure factor calculated from a superposition of isolated spherical atoms with positional and thermal parameters essentially free from the bias due to the nonspherical electron redistribution upon bond formation. In the absence of a set of atomic parameters from an independent neutron diffraction experiment, the least biased parameters for stishovite represent those obtained by the population and κ refinement described above.

The difference, or so-called deformation, electron density in an axial/equatorial bond plane of the octahedron, and in a section through the equatorial plane of the oxygen atoms, is given in Figs. 2 and 3, respectively. Both maps were calculated with the computer program FOPROP (*42*) using atomic parameters from the full-data population and κ refinement, but including only those data with sin $\theta/\lambda < 1.0$ Å^{-1}. The average standard deviation of the observed electron density at a general position in the unit cell was estimated (*43*) to be 0.031 e Å^{-3} for the same data cutoff (0.047 e Å^{-3} for all the data), and residual electron density features of magnitude greater than about 0.1 e Å^{-3} may therefore be considered to be significant.

The most striking features of these maps are the residual peaks of electron density located along the two kinds of silicon–oxygen bonds. The bonds to the axial, O_a, and equatorial, O_e, oxygen atoms have maximum densities of 0.29 and 0.47 e Å^{-3}, respectively, with the shorter equatorial bonds possessing the larger peak maxima. Also, as is typical of a material with polar covalent bonds, both bond maxima are significantly closer to the more electronegative O atom than to Si.

The comparable features of these chemically, but not crystallographically, equivalent Si–O bond peaks lends considerable support to the accuracy of the results and to the conclusion that they represent an accumulation of covalent-bond electron density.

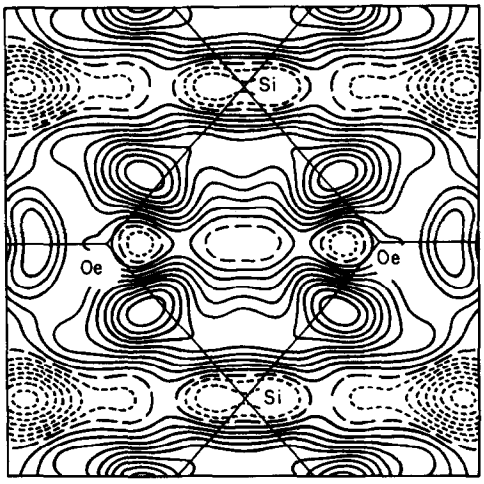

FIG. 3. Experimental deformation density map for the coordination plane of the oxygen atom in stishovite. Calculated and presented as for Fig. 2.

In fact, peaks of similar magnitude have been observed between (tetrahedrally coordinated) Si and O atoms in olivines and pyroxenes (*44*), low quartz (*45*), silicate spinels (*46*), pectolite (*47*), and coesite (*30*). The results for 6-coordinated Si in stishovite therefore contrast with the observation of a significant *decrease* in the covalency of Al–O bonds (as measured by residual electron densities) in passing from 4 coordination in berlinite (*48*) to 6 coordination in $CoAl_2O_4$ (*49*) and diaspore (*32*). It is worth noting, however, that the equivalent isotropic thermal parameter[3] for the Si atom in stishovite is less than half the average magnitude of the corresponding Al or Si parameters in the other compounds listed, while the value for the O atom in stishovite is smaller by a factor of 3. Indeed, the stishovite values are also smaller than the typical thermal vibration parameters of molecular compounds determined at low (i.e., liquid N_2 or He) temperature. For stishovite, the markedly smaller thermal vibration is no doubt a function of its high density, relative to the other compounds, brought about by the high synthesis pressure of 90 kbar. As a result, the electron density is not as severely smeared by thermal effects and the residual peaks may therefore by expected to appear as sharper, more pronounced features, as in the deformation maps of Figs. 2 and 3.

Perhaps the most intriguing features of the electron density maps are those in the equatorial plane of the SiO_6 octahedron (Fig. 3). Whereas the bond peaks in the axial/equatorial plane of Fig. 2 are well separated features, the maxima in the equatorial bonds are connected by bridges of electron density of magnitude approximately half that of the bonds themselves. Indeed, these bridges of electron density are considered to be energetically favorable due to their shielding effect and consequent reduction of repulsive forces between the Si atoms in the edge-sharing octahedra of the structure (*50*). Note also that whereas the axial bond density maximum lies centrally disposed about the bond axis in Fig. 2, the equatorial bond maxima in Fig. 3 are displaced outwards from the shared edge, probably reflecting strain in the four-membered ring system.

[3] Defined as the cube root of the product of the anisotropic temperature factor coefficients U_{ii}, $i = 1$–3.

Molecular Orbital Calculations on Molecules with 4- and 6-Coordinate Silicon

The Shape of the SiOSi Group in Molecules and Solids with 4-Coordinate Si

Studies of the disiloxy SiOSi group have shown that its shape is essentially the same regardless of whether the group occurs in a gas phase molecule or in a molecular crystal (*4, 5*). Moreover, the group's shape is indicated to persist even in silicate minerals, suggesting that the forces that govern its geometry in a molecule prevail even in the solid state. Because of this likelihood, several workers (*51, 52*) have argued that molecular orbital (MO) studies on siloxane and silicate molecules can be used to improve our understanding of the shape and charge density distribution of the group in a silicate mineral. In exploring this possibility, Newton and Gibbs (*53*), Gibbs *et al.* (*4, 5*), Meagher *et al.* (*54*), and Chakoumakos *et al.* (*55*) have analyzed the configuration and energetics of the SiOSi group in a variety of siloxane and silicate molecules with *ab initio* MO theory and have obtained a quantitative account of the bonding in solid silicates and siloxanes. In particular, this includes (i) a mimicking of the experimental correlations between Si–O bond length, SiOSi angle, and the total bond strength sum reaching the oxygen atom bonded to Si, (ii) the generation of the Brown–Shannon bond length versus bond strength curves for *M*–O bonds involving

first and second row M atoms, (iii) the successful calculation of the bulk modulus of α-quartz, and (iv) the computer simulation of SiO_2 in the α-quartz and α-cristobalite structures. In short, MO studies of silicic acid and siloxane molecules containing 4-coordinated Si are indeed capable of mimicking experimental trends and static properties of silicates. An examination of the resulting wave functions and potential energy surfaces has also provided new insights into the energetics and the nature of bonding in the SiOSi group.

Optimization of the Si–O Bond Length for 6-Coordinated Si in $(\frac{2}{3}H)_{12}SiO_6$

It is noteworthy that the Si–O bond lengths (1.77–1.79 Å) recorded for two recently refined molecular crystals with 6-coordinate Si (*19*) lie in the range of bond lengths (1.72–1.80 Å) recorded for silicates with 6-coordinate Si. In view of this close agreement, we completed a series of MO calculations on a neutral 6-coordinate $(\frac{2}{3}H)_{12}SiO_6$ molecule with T_h point symmetry (where "$\frac{2}{3}$ H" refers to a hydrogen-like atom with a core charge of two thirds as described below) to explore how well its calculated geometry mimics the Si–O bond lengths in stishovite as well as those in other silicates with 6-coordinate Si. The assignment of an effective core charge of two thirds to the hydrogen-like atom allows the molecule to be charge neutral and also allows the proper bond strength relationships to be maintained, i.e., the sum of the bond strengths reaching each oxygen atom is exactly 2.0 as required by Pauling's electrostatic valence rule (this is based on a nominal population of two thirds of an electron on each hydrogen-like atom).

In contrast to the molecule with T_h symmetry, we have also generated a second molecule with the same topology but with D_{2h} point symmetry which matches the stishovite structure more closely. However, because this model required four of the hydrogen-like atoms to be in rather close proximity, we have chosen not to use this structure for geometry optimization. In a later section, we will use this more realistic model to calculate the deformation density. The Si–O bond length of the T_h molecule (Fig. 4) was optimized in a minimal basis STO-3G MO calculation. The potential energy curve for the molecule calculated as a function of the Si–O bond length is compared in Fig. 5 with a histogram of 41 observed bond lengths from silicates with 6-coordinated Si (the average bond length for this distribution (1.76 Å) is within 0.03 Å of the minimum energy value of 1.73 Å). The quadratic stretching force constant calculated from the curvature of the potential energy curve is 520 N m^{-1}, about 10% less than that calculated for the 4-coordinated Si atom in monosilicic acid, H_4SiO_4 (*4*). The smaller force constant of the Si–O bond in

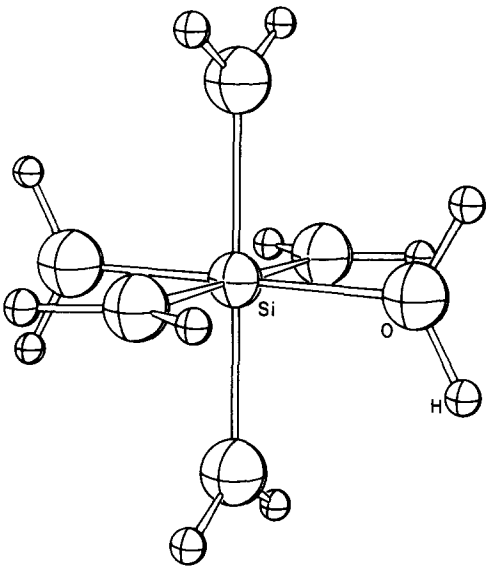

FIG. 4. Diagram of the $(\frac{2}{3}H)_{12}SiO_6$ molecule (T_h point symmetry) used in STO-3G molecular orbital calculations of the optimal Si–O bond length for 6-coordinated Si. The central sphere is Si, the large spheres are O, and the small spheres are hydrogen-like atoms (as defined in text and Fig. 9 caption). No significance is attached to the relative sizes of the spheres used to represent the atoms in this figure and Figs. 8 and 9.

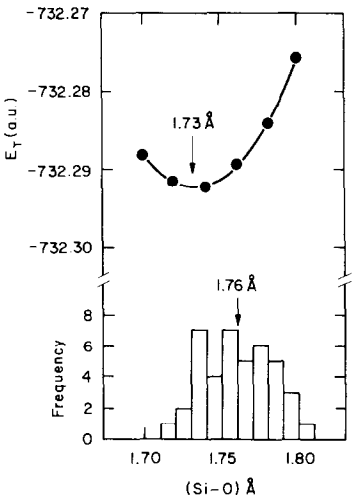

FIG. 5. A potential energy curve calculated for the molecule $(\frac{2}{3}\ H)_{12}SiO_6$ (see Fig. 4) as a function of the Si–O bond length (Si–O). In the calculation of the total energy E_T all (Si–O) values were considered as equivalent. A frequency distribution of 41 experimental Si–O bond lengths in silicates and siloxane molecular crystals with 6-coordinated silicon is superimposed on the drawing. The average bond length for the observed bond length distribution is 1.76 Å compared with a minimum energy bond length of 1.73 Å.

the molecule with 6-coordinated Si is consistent with its longer length and the larger coordination number of Si.

Dependence of Charge and Si–O Bond Length on Coordination Number

The charge, Q(Si), calculated for the Si atom in the $(\frac{2}{3}\ H)_{12}SiO_6$ molecule (+1.51 *e*) in Fig. 4 using a STO-3G basis is ≈0.2 *e* larger than that (+1.36 *e*) calculated for H_4SiO_4 (*53*). The pertinent charges are presented in Table IV which also includes the charges obtained with larger basis sets. The charges calculated with the split valence basis will be discussed in the last section of this paper in conjunction with the calculated deformation density. In contrast with the STO-3G charges, the net atomic charge obtained for Si in the least-squares refinement of the crystal structure of stishovite, Q(Si) = +1.71 *e* (Tables III and IV), is indicated to be ~0.7 *e* larger than that refined experimentally for the 4-coordinate Si atoms in the other silica polymorphs (0.9 to 1.0 *e*). In view of the smaller difference between the calculated charges, we optimized the Si–O bond lengths for three additional molecules (linear SiO and SiO_2, and planar H_2SiO_3), so that the relationship between the charge and coordination number of Si could be examined in more detail. For the H_2SiO_3 molecule, the OSiO angles were fixed at $\cos^{-1}(-\frac{1}{2})$, the SiOH angles were fixed at $\cos^{-1}(-\frac{1}{3})$, and the OH bonds were set in the plane of the molecule with a length of 0.96 Å. The optimized Si–O bond lengths of the three molecules and those for H_4SiO_4 and $(\frac{2}{3}H)_{12}SiO_6$ are plotted against the coordination number of Si, CN(Si), in Fig. 6. The trend between these two param-

TABLE IV

EXPERIMENTAL AND THEORETICAL NET ATOMIC CHARGES (*e*) FOR THE ATOMS IN α-QUARTZ AND STISHOVITE

	α-quartz (60)		H_4SiO_4	
		STO-3G	STO-3G*	66-31G*
Q(Si)	+1.0	1.36	0.81	1.10
Q(O)	−0.5	−0.52	−0.40	−0.72
	Stishovite (this study)		$(\frac{2}{3}\ H)_{12}SiO_6$[a]	
		STO-3G	STO-3G*	66-31G*
Q(Si)	+1.71	1.51	0.87	1.78
Q(O)	−0.86	−0.54	−0.46	−0.99

[a] Calculated for the $(\frac{2}{3}\ H)_{12}SiO_6$ molecule depicted in Fig. 4.

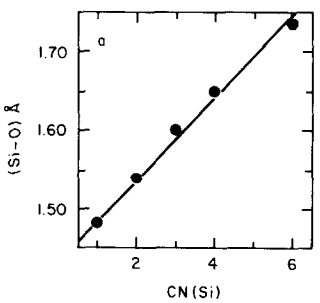

FIG. 6. STO-3G optimized Si–O bond lengths versus Si coordination number CN(Si) for the molecules SiO, SiO_2, H_2SiO_3, H_4SiO_4, and $(\frac{2}{3}\ H)_{12}SiO_6$.

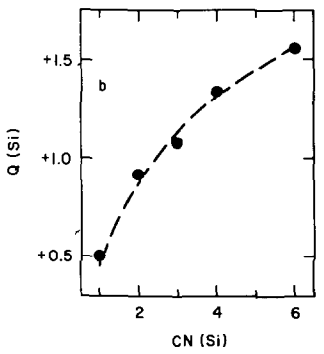

FIG. 7. STO-3G calculated charges on the Si atom Q(Si) versus Si coordination number CN(Si) for the molecules SiO, SiO_2, H_2SiO_3, H_4SiO_4, and $(H)_{12}SiO_6$.

eters is indicated to be linear (with a correlation coefficient of 0.995) in agreement with several such trends reported by Shannon and Prewitt (*41*). On the other hand, the trend between CN(Si) and Q(Si) is indicated to be nonlinear (Fig. 7) with the largest increase in Q(Si) involving the smaller coordination numbers and the smallest increase involving the larger coordinations. Nonetheless, the calculations indicate, as suggested earlier, that the ionicity of the bond increases with coordination number and Si–O bond length.

Note that both the experimentally determined Si charge, and the STO-3G estimate, are less than half the magnitude of the charge corresponding to a completely ionic model, thereby supporting the postulate that molecular charge distributions tend toward electroneutrality (*56, 57*). Moreover, as expected, the Si atom is contracted ($\kappa > 1$ as shown in Table III) relative to an isolated Hartree–Fock atom, whereas the negative O atom is expanded ($\kappa < 1$), in agreement with Slater's rules for atomic screening factors.

Previous experimental estimates of the atomic charge of Si in oxides are few in number and have been restricted to those compounds in which the atom is tetrahedrally coordinated. Although the net charge on Si for the silicates in general shows a wide variation up to +2.7 *e* (*44–47, 58, 59*), we note that when the influence of other cations can be ignored, as in the case of the SiO_2 polymorphs, the charges on the Si atoms appear to be much closer to electroneutrality. For example, in coesite (*30*) the two Si atoms have charges of +0.9(3) and +0.8(3) *e*, while in low quartz (*60*), the charge is +1.0(1) *e*. Therefore, using the definition of experimental ionicity as the ratio of actual charge to formal charge (*60*), the ionicity of the Si–O bond is indicated to change from a value near 25% in the case of tetrahedral coordination (where the mean bond length is around 1.61 Å) to a value near 40% for octahedral coordination (mean bond length around 1.76 Å).

Octahedral Shared Edge Distortions in $Si_2(OH)_2F_8^{2-}$

As discussed earlier, each Si-containing octahedron in stishovite shares 2 of its 12 edges with adjacent octahedra and, as expected, these edges are the shortest O . . . O contacts in the structure. The sharing of edges between cation-containing polyhedra and their shortening relative to the unshared edges are features common to many solids. However, according to Pauling (*39*), a structure is destabilized by the presence of shared edges, the effect being greatest for cations with large ionic valence and small coordination number. This rule, known as his third rule, was deduced from the ionic model and has since been used to account for polyhedral distortions in a large number of solids. Nevertheless, recent molecular orbital studies (*61, 62*) of shared edge distortions in molecules indicate that an important determinant of the total energy of the shared edge configuration is the antibonding interactions between juxtaposed metal atoms on opposite sides of the shared edge. In other words, antibonding rather than ionic repulsions may be responsible, in large part, for increasing the metal–

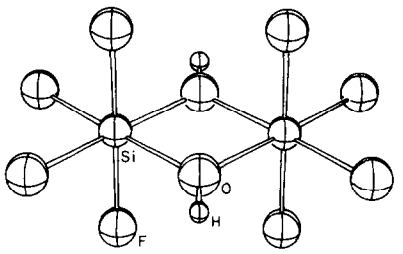

FIG. 8. Diagram of the $Si_2(OH)_2F_8^{2-}$ molecule used in STO-3G molecular orbital calculations of the optimal geometry of the shared edge between two octahedrally coordinated Si atoms.

metal separation and for shortening the shared edge length. In contradiction to the ionic model, this result suggests that the degree to which a shared edge is shortened may be a measure of the antibonding interaction between the metal atoms, the greater the interaction, the shorter the edge.

In our study of the shared edge configuration in stishovite, we optimized the geometry of the shared edge molecule $Si_2(OH)_2F_8^{2-}$ (Fig. 8) with STO-3G MO calculations. The topology of the shared edge was assumed to consist of two oxygen atoms each bonded to two silicon atoms and one hydrogen. The hydrogen atom was located in the SiOSi plane at a fixed distance of 0.96 Å from the oxygen. The octahedral coordination of each Si was completed by four additional fluorine atoms with each FSiF angle fixed at 90°. Optimization of the Si–F bond lengths yielded a value of 1.66 Å in agreement with an experimental value (1.64 Å) reported for 6-coordinated Si in the molecular crystal tetrafluorobispyridinesilicon (*63*). The optimized geometry of the shared edge of the molecule is compared with that observed for stishovite in Table V. Despite the long-range Madelung potential in the solid and the necessary substitution of several O ions by F to permit the calculations to be undertaken, the angles calculated for the molecule agree to within about 8° of the observed value, and the calculated Si–O bond lengths agree within 0.05 Å. On the other hand, the calculated value of the shared edge is 0.13 Å shorter than that observed in stishovite. Nonetheless, the overall configuration of the optimized geometry of the shared edge in the molecule is in reasonably good agreement with that observed for stishovite.

TABLE V

BOND LENGTHS AND ANGLES FOR THE SHARED EDGE CONFIGURATION OF THE MOLECULE $Si_2(OH)_2F_8^{2-}$

Parameter	Calculated[a]	Observed[b]
d(Si–O)	1.80 Å	1.757 Å
d(O . . . O)	2.16 Å	2.290 Å
OSiO	73°	81.3°
SiOSi	106°	98.7°

[a] Calculated with STO-3G MO theory.

[b] Equivalent observed parameters in stishovite.

Theoretical Deformation Maps of the Si–O Bonds for 4- and 6-coordinate Si

In devising a suitable molecular model for theoretical charge density calculations relevant to stishovite, we considered the following factors: (i) adequate flexibility of the atomic orbital (AO) basis set, (ii) simulation of the bonding environment of both the Si and O atoms, and (iii) computational feasibility. Although a previous study has shown that a minimal atomic orbital basis set (i.e., the STO-3G basis) may in some cases yield useful qualitative charge density distributions pertinent to silica (*53*), a more flexible basis is necessary in general for reliable results. Studies on disiloxane (*64, 65*) suggest that a so-called split valence *s,p* basis (i.e., a minimal basis for core electrons, and two sets of valence *s* and *p* functions) on Si and O, coupled with a set of 3*d* polarization functions on Si, yields quantitatively meaningful deformation densities in the Si–O bond region. If detailed information is required in the immediate vicinity of

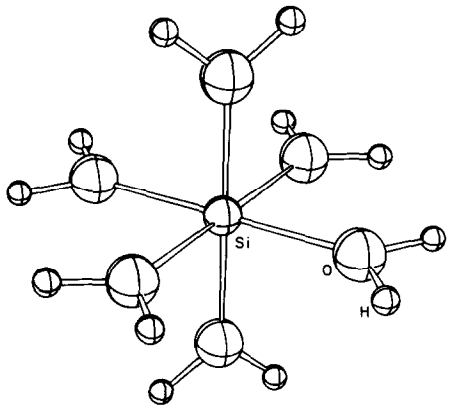

FIG. 9. Diagram of the $(\frac{2}{3}\ H)_{12}SiO_6$ octahedral molecule (D_{2h} point symmetry) used in split valence 66-31G* basis molecular orbital calculations of the deformation electron density in the Si–O bond for 6-coordinated Si. The central sphere is Si, and the large and small spheres on the periphery of the cluster are O and "$\frac{2}{3}$ H" hydrogen-like atoms, respectively. The hydrogen-like atoms have been assigned a core charge of two thirds, so that the molecule is neutral and the sum of bond strengths reaching each oxygen is exactly 2.0. The bond angles associated with the hydrogen-like atoms are the same as the corresponding SiOSi angles in stishovite (Fig. 1) with the exception of the four hydrogen-like atoms used to mimic the two Si atoms opposite the shared edges at $\frac{1}{2}$, $\frac{1}{2}$, $\pm\frac{3}{2}$. To avoid undue steric repulsions, the HOSi angles were set at 130° instead of 100° observed for the corresponding SiOSi angle in stishovite.

the O atoms, it is necessary to place a set of 3*d* orbitals on O as well. This was not done in obtaining the results reported below, since the primary focus is on the Si–O bond densities.

The following calculations used the split valence 66-31G* basis with *d* orbitals[4] on Si and were completed on the D_{2h} molecule (Fig. 9) based on the stishovite structure as discussed above. The calculated deformation map through the equatorial SiO_4 group of this molecule is presented in Fig. 10, and is seen to correspond closely in many respects to the experimental map in Fig. 2.

[4] We used a preliminary version of this basis set. The results are essentially the same as those obtained from the final version of the basis set (*66*).

For comparison, an analogous map through an SiO_2 group of the H_4SiO_4 molecule (a model for tetravalent Si and divalent O) is given in Fig. 11. The peak values of the calculated deformation densities in the Si–O bond regions are 0.26 *e* Å^{-3} for $(\frac{2}{3}\ H)_{12}SiO_6$ and 0.33 *e* Å^{-3} for H_4SiO_4, somewhat less than the observed values (Figs. 2 and 3), which average out at 0.38 *e* Å^{-3}. Moreover, both calculated and experimental bond density maxima are appreciably shifted from the Si–O bond midpoint toward the oxygen, as expected from electronegativity considerations. Therefore, in spite of the limitations of the orbital basis set and the discrete molecular model in the case of the calculated data, and the different degrees of thermal smearing, presence of different cations, etc., in the case of the observed data, both theory and experiment are in quite reasonable agreement and give strong indications of partial covalency in Si–O bonding associated with 6-coordinated, as well as 4-coordinated, silicon.

Finally, it is noteworthy that the atomic

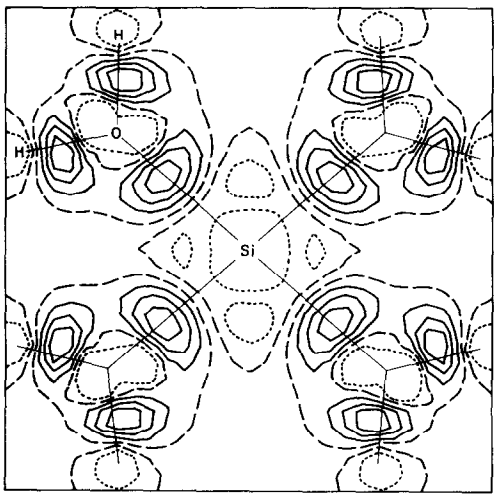

FIG. 10. Split valence basis deformation density map calculated through the SiO_4 group of the $(\frac{2}{3}\ H)_{12}SiO_6$ molecule displayed in Fig. 9. The contour interval is 0.07 *e* Å^{-3} with all negative contours deleted except the first.

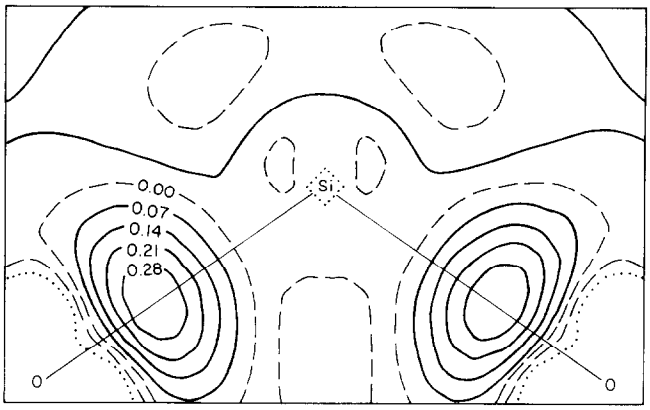

FIG. 11. Split valence basis deformation density calculated for one of the SiO_2 groups in the molecule H_4SiO_4. The contour interval is 0.07 $Å^{-3}$ with all negative contours deleted except the first.

charge on 6-coordinate Si provided by these more sophisticated split valence calculations (Table IV) is ~0.7 *e* larger than that (1.10 *e*) provided by a comparable calculation for H_4SiO_4 (*53*). This increase in Q(Si) with increase in coordination number from 4 to 6 compares well with an increase of ~0.7 *e* recorded in the least-squares refinement of the materials with 4- and 6-coordinate Si discussed earlier. Moreover, in agreement with the earlier calculations on H_4SiO_4 and $H_6Si_2O_7$ (*53*), the ratio of the charges on Si and O in $(\frac{2}{3}\ H)_{12}SiO_6$ determined with the split valence basis is approximately 2 : 1 (Table IV), the expected ratio for a silicate, despite the lack of constraints in the calculations.

Acknowledgments

The authors are indebted to Dr. G. M. McLaughlin of the Research School of Chemistry at the Australian National University for his painstaking care during data collection, to Dr. M. A. Spackman for his able assistance during the monopole refinement, and to the Research Division of VPI and SU for contributing large sums of money to help defray the computing costs. We are especially pleased to thank the National Science Foundation for Grant EAR 77-23114 awarded to GVG and Professor P. H. Ribbe to study bonding in minerals, and the U.S. Department of Energy supported by its Office of Basic Energy Sciences for Contract DE-AC02-76CH00016 awarded to MDN.

References

1. D. L. GRISCOM, *J. Non-Cryst. Solids* **24,** 155 (1977).
2. K. HUBNER, *Phys. Status Solidi A* **40,** 133 (1977).
3. S. T. PANTELIDES, "The Physics of SiO_2 and its Interfaces," Pergamon, New York (1978).
4. G. V. GIBBS, E. P. MEAGHER, M. D. NEWTON, AND D. K. SWANSON, *in* "Structure and Bonding in Crystals" (M. O'Keeffe and A. Navrotsky, Eds.), p. 195, Academic Press, New York (1981).
5. G. V. GIBBS, *Amer. Mineral.* **67,** 421 (1982).
6. S. M. STISHOV AND S. V. POPOVA, *Geokhimya* **10,** 837 (1961).
7. E. C. T. CHAO, J. J. FAHEY, J. LITTLER, AND E. J. MILTON, *J. Geophys. Res.* **67,** 419 (1962).
8. A. E. RINGWOOD, "Composition and Petrology of the Earth's Mantle," McGraw-Hill, New York (1975).
9. A. E. RINGWOOD, A. F. REID, AND A. D. WADSLEY, *Acta Crystallogr.* **23,** 1093 (1967).
10. A. F. REID AND A. E. RINGWOOD, *J. Solid State Chem.* **1,** 6 (1969).
11. A. E. RINGWOOD, *Earth Planet. Sci. Lett.* **2,** 255 (1967).
12. T. YAGI, H. K. MAO, AND P. M. BELL, *Phys. Chem. Miner.* **3,** 97 (1978).
13. J. J. FLYNN AND F. P. BOER, *J. Amer. Chem. Soc.* **91,** 2756 (1969).
14. G. BISSERT AND F. LIEBAU, *Acta Crystallogr. Sect. B* **26,** 233 (1970).
15. R. A. EDGE AND H. F. W. TAYLOR, *Acta Crystallogr. Sect. B* **27,** 594 (1971).
16. K. F. HESSE, *Acta Crystallogr. Sect. B* **25,** 724 (1979).
17. R. D. SHANNON, J. CHENAVAS, AND J. C. JOUBERT, *J. Solid State Chem.* **12,** 16 (1975).

18. F. LIEBAU, in "Handbook of Geochemistry" (K. H. Wedepohl, Ed.), Chap. 14A, Springer-Verlag, Berlin (1972).
19. T. ADAMS, T. DEBAERDEMAKER, AND U. THEWALT, "Collected Abstracts 5th European Crystallographic Metting," Copenhagen, 32S (1979).
20. S. M. STISHOV AND N. V. BELOV, *Dokl, Acad. Nauk SSSR* **143,** 951 (1962).
21. A. PREISINGER, *Naturwiss.* **49,** 345 (1962).
22. W. H. BAUR AND A. A. KHAN, *Acta Crystallogr. Sect. B* **27,** 2133 (1971).
23. W. SINCLAIR AND A. E. RINGWOOD, *Nature (London)* **272,** 714 (1978).
24. P. COPPENS, T. N. GURU ROW, P. LEUNG, E. D. STEVENS, P. J. BECKER, AND Y. W. YANG, *Acta Crystallogr. Sect. A* **35,** 63 (1979).
25. H. ITO, K. KAWADA, AND S. AKIMOTO, *Phys. Earth Planet Int.* **8,** 277 (1974).
26. J. HORNSTRA AND B. STUBBE, "PW1100 Data Processing Program," Philips Res. Lab., Eidhoven, Holland (1972).
27. J. M. STEWART (ED.), "The XRAY System—Version of 1976," Tech. Rept. TR-446, Computer Science Center, Univ. of Maryland, College Park, Md. (1976).
28. J. A. IBERS AND W. C. HAMILTON (Eds.), "International Tables for X-ray Crystallography," Vol. IV, Kynoch, Birmingham (1974).
29. P. COPPENS AND W. C. HAMILTON, *Acta Crystallogr. Sect. A* **26,** 71 (1970).
30. G. V. GIBBS, R. J. HILL, F. K. ROSS, AND P. COPPENS, *Geol. Soc. Amer. Abstr. Progr.* **10,** 407 (1978).
31. R. J. HILL, J. R. CRAIG, AND G. V. GIBBS, *J. Phys. Chem. Solids* **39,** 1105 (1978).
32. R. J. HILL, *Phys. Chem. Miner.* **5,** 179 (1979).
33. P. COPPENS, *Angew. Chem. Int. Ed. Engl.* **16,** 32 (1977).
34. W. C. HAMILTON, *Acta Crystallogr.* **18,** 502 (1965).
35. L. VEGARD, *Phil. Mag.* **32,** 65 (1916).
36. C. K. JOHNSON, "ORTEP-II: A FORTRAN Thermal-Ellipsoid Plot Program for Crystal Structure Illustrations," U.S. Nat. Tech. Inf. Serv., ORNL-5138, Oak Ridge, Tenn. (1976).
37. D. B. ROGERS, R. D. SHANNON, A. W. SLEIGHT, AND J. L. GILLSON, *Inorg. Chem.* **8,** 841 (1969).
38. W. H. BAUR, *Acta Crystallogr. Sect. B* **32,** 2200 (1976).
39. L. PAULING, "The Nature of the Chemical Bond," 3rd ed., Cornell Univ. Press, Ithaca, New York (1960).
40. W. H. BAUR, *Acta Crystallogr.* **14,** 209 (1961).
41. R. D. Shannon and C. T. Prewitt, *Acta Crystallogr. Sect. B* **25,** 925 (1969).
42. R. F. STEWART AND M. A. SPACKMAN, private communication (1981).
43. E. D. STEVENS AND P. COPPENS, *Acta Crystallogr. Sect. A* **32,** 915 (1976).
44. K. FUJINO, S. SASAKI, Y. TAKEUCHI, AND R. SADANAGA, *Cryst. Soc. Jpn Ann. Mtg.,* 76 (1976).
45. Y. LEPAGE AND G. DONNAY, *Acta Crystallogr. Sect. B* **23,** 2456 (1976).
46. F. MARUMO, M. ISOBE, AND S. AKIMOTO, *Acta Crystallogr. Sect. B* **33,** 713 (1977).
47. Y. TAKEUCHI AND Y. KUDOH, *Z. Krist.* **146,** 231 (1977).
48. N. THONG AND D. SCHWARZENBACK, *Acta Crystallogr. Sect. A* **35,** 658 (1979).
49. K. TORIUMI, M. OZIMA, M. AKAOGI, AND Y. SAITO, *Acta Crystallogr. Sect. B* **34,** 1093 (1978).
50. J. A. TOSSELL AND G. V. GIBBS, *Phys. Chem. Min.* **2,** 21 (1977).
51. G. V. GIBBS, M. M. HAMIL, S. J. LOUISNATHAN, L. S. BARTELL, AND H. YOW, *Amer. Mineral.* **57,** 1578 (1972).
52. J. A. TOSSELL AND G. V. GIBBS, *Acta Crystallogr. Sect. A* **34,** 463 (1978).
53. M. D. NEWTON AND G. V. GIBBS, *Phys. Chem. Miner.* **6,** 221 (1980).
54. E. P. MEAGHER, D. K. SWANSON, AND G. V. GIBBS, *EOS* **61,** 408 (1980).
55. B. C. CHAKOUMAKOS, R. J. HILL, AND G. V. GIBBS, *Amer. Mineral.* **66,** 1237 (1981).
56. L. PAULING, *J. Chem. Soc. (London),* 1461 (1948).
57. J. C. SLATER, "Quantum Theory of Molecules and Solids," Vol. 2, McGraw-Hill, New York (1965).
58. S. SASAKI, K. FUJINO, Y. TAKEUCHI, AND R. SADANAGA, "XIth IUCr Congress," Abstr. S21, Warsaw (1978).
59. R. C. PETERSON, G. V. GIBBS, AND F. K. ROSS, *Geol. Soc. Amer. Abstr. Progr.* **12,** 498 (1980).
60. R. F. STEWART, M. A. WHITEHEAD, AND G. DONNAY, *Amer. Mineral.* **65,** 324 (1980).
61. J. A. TOSSELL AND G. V. GIBBS, *Amer. Mineral.* **61,** 287 (1976).
62. T. J. MCLARNAN, R. J. HILL, AND G. V. GIBBS, *Aust. J. Chem.* **32,** 949 (1979).
63. V. A. BAIN, R. C. G. KILLEAN, AND M. WEBSTER, *Acta Crystallogr. Sect. B* **25,** 156 (1969).
64. M. D. NEWTON AND G. V. GIBBS, in preparation.
65. J. W. DOWNS, R. J. HILL, M. D. NEWTON, J. A. TOSSELL, AND G. V. GIBBS, in "Electron Distributions and the Chemical Bond," (D. Coppens and M. B. Hall, Eds.), Plenum, New York (1981).
66. M. S. GORDON, J. S. BRINKLEY, J. A. POPLE, W. J. PIETRO, AND W. J. HEHRE, *J. Amer. Chem. Soc.* **104,** 2797 (1982).